ACS APPLIED BIO MATERIALS

www.acsabm.org

Article

In Vivo Capsid Engineering of Bacteriophages for Oriented Surface Conjugation

Kathryn A. Hufziger,[†] Emma L. Farquharson,[†] Brenda G. Werner, Qingmin Chen, Julie M. Goddard, and Sam R. Nugen*

Cite This: *ACS Appl. Bio Mater.* 2022, 5, 5104−5112

Read Online

ACCESS | Metrics & More | Article Recommendations | Supporting Information

ABSTRACT: The current state-of-the-art in bacteriophage (phage) immobilization onto magnetic particles is limited to techniques that are less expensive and/or facile but nonspecific or those that are more expensive and/or complicated but ensure capsid-down orientation of the phages, as necessary to preserve infectivity and performance in subsequent applications (e.g., therapeutics, detection). These cost, complexity, and effectiveness limitations constitute the major hurdles that limit the scale-up of phage-based strategies and thus their accessibility in low-resource settings. Here, we report a plasmid-based technique that incorporates a silica-binding protein, L2, into the T7 phage capsid, during viral assembly, with and without inclusion of a flexible linker peptide, allowing for targeted binding of the phage capsid to silica without requiring the direct modification of the phage genome. L2-tagged phages were then immobilized onto silica-coated magnetic nanoparticles. Inclusion of the flexible linker between the phage capsid protein and the L2 protein improved immobilization density compared to both wild type T7 phages and L2-tagged phages without the flexible linker. Taken together, this work demonstrates phage capsid modification without engineering the phage genome, which provides an important step toward reducing the cost and increasing the specificity/directionality of phage immobilization methods and could be more broadly applied in the future for other phages for a range of other capsid tags and nanomaterials.

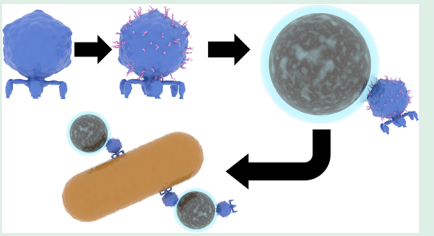

KEYWORDS: *T7, in vitro phage engineering, silica binding, magnetic nanoparticles, phage technology, tailed phages, plasmid-based capsid tagging*

INTRODUCTION

Bacterial contamination of food[1−7] and water[8,9] remains a global burden to human health with economic impacts including medical costs, lost productivity, and food waste from bacterial-derived spoilage and contamination.[2,10−13] Phages are obligate parasites that can only replicate within specific bacterial hosts.[14,15] For tailed phages, the evolution of highly specific interactions between tail fibers and targeted bacterial surface receptors has allowed phages to identify hosts while minimizing cross-reactivity in complex environments.[16−18] Thus, phage-based technologies enable accurate, rapid, and practical detection tools with broad applications in food and water safety,[1,19,20] medical diagnostics,[21] and environmental monitoring.[22]

Recent reviews[1,21,23−29] have surveyed phage-based bacterial detection methods, with some presenting limit of detection (LOD) values of <10 CFU/mL in <10 h.[1,19] Immobilization of the phages onto magnetic micro- or nanoparticles can permit preconcentration of the bacteria, further reducing LOD values. Immobilization of phages onto magnetic particles has been accomplished with methods that include amide bonds formed by carboxylic acid−amine coupling,[30−33] interaction of streptavidin with biotin,[34−36] electrostatic interactions,[37,38] and unnatural amino acids such as alkynes.[19] However, each of these methods suffers from at least one of the following limitations: cost, complexity, or effectiveness. The simpler methods (amide bonds and electrostatic interactions) are nonspecific and cannot ensure capsid-down orientation of the immobilized phages, a necessity for maintaining their binding specificity. In contrast, methods that do ensure the proper orientation of phages (streptavidin−biotin and unnatural amino acids) require more costly materials and/or complicated, labor-intensive molecular engineering techniques.[39] These limitations present a hurdle to pragmatic scalability of phage−nanoparticle conjugates for bacteria detection, especially for low-resource settings which the United Nations estimated will comprise >60% of the global population by 2050.[40] To enable point-of-care and point-of-use testing in these areas, considerations of cost and pragmatism are necessary in design of detection systems.

To permit dispersion and prevent agglomeration, magnetic nanoparticles (MNPs) can be coated with an inert material, with silica decoration a common and economic option.

Received: May 11, 2022
Accepted: October 12, 2022
Published: October 20, 2022

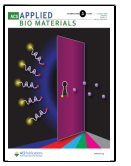

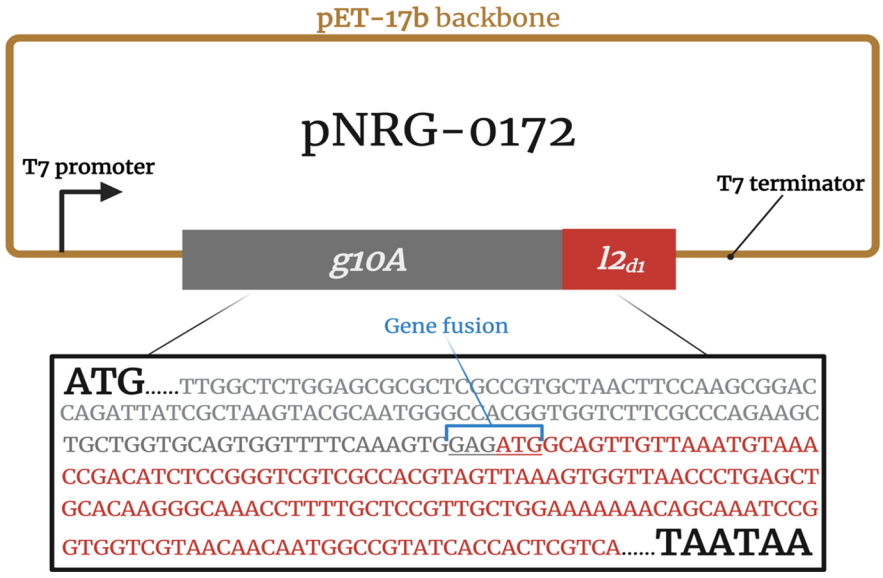

Figure 1. Graphical representation of pNRG-172. The coding regions of *g10A* and $l2_{d1}$ were fused by removing the stop codon from *g10A* and adding a double stop codon at the end of $l2_{d1}$.

Current methods for binding phages to silica include silane modification to introduce functional groups that either couple to the phage via primary amines present throughout the outer protein shell (including both the capsid and tail fibers) or modify the silica charge to promote favorable electrostatic interactions between phages and the silica surfaces.[41−43] Unfortunately, these nonspecific methods can lead to improper orientation of the phages such that the tails may no longer be able to seek out and bind their bacterial targets. An improved method for binding phages to magnetic silica particles would modify the phage capsids with a silica-targeting group, permitting directed conjugation of the phages to the particles through their capsids.

L2, a ribosomal protein from *Escherichia coli*, has been shown to bind strongly to silica and has been successfully used as a silica-binding tag in fusion proteins.[44−46] L2 is 273 residues long with a net positive charge at pH 7. At pH > 7, L2 has a high affinity for silica surfaces, where there are electrostatic interactions between deprotonated, and thus negatively charged, silanol groups and the net-positively charged L2 domain 1 ($L2_{d1}$; residues 1−60) and L2 domain 3 ($L2_{d3}$; residues 203−273).[44,46] L2 domain 2 does not contribute to silica binding.[44,46] L2 has also been shown to bind to silica even in the presence of high concentrations of salt, suggesting that, in addition to electrostatic interactions, the intrinsic disorder of the N- and C-terminal ends of L2 allows nonpolar groups in these regions to interact with hydrophobic siloxane groups on silica surfaces.[47]

To overcome challenges in site-directed coupling of phage onto silica decorated MNPs, we developed a plasmid-based technique which incorporates L2 into the major capsid protein (Gp10A) of T7 phages without requiring the direct modification of the T7 genome. We used T7 as the model phage for this work due to its history of use in the field of phage display and the many previous reports of successful incorporation of proteins into T7's assembled procapsid.[48] T7 is also of particular interest as a detection tool due to its short replication time (17−25 min[49−51] using common strains of *E. coli*[52]), formation of visible plaques within 3 h (at 37 °C), ability to lyse hosts in liquid culture within 1−2 h, and ability to release ∼100 progeny per infected bacterium under optimal conditions.[49] Further, T7 is stable over a wide pH range but infects best when the pH value is between 6 and 8.[53] Genome replication, gene expression, protein synthesis, and viral assembly happen simultaneously during T7 infection, where progeny are assembled by selecting structural subunits from pools of overexpressed proteins, which in this work allows L2-tagged capsid proteins to be assembled on the T7 capsid.[51]

In this work, we produced three L2-tagged T7 mutants by engineering the Gp10A capsid protein with $L2_{d1}$ and $L2_{d3}$, with and without the incorporation of a flexible linker (L-). Mutant phages are denoted as $T7_{L2d1}$ (incorporating Gp10A-$L2_{d1}$), $T7_{L\text{-}L2d1}$ (incorporating Gp10A-L-$L2_{d1}$), and $T7_{L\text{-}L2d1d3}$ (incorporating Gp10A-L-$L2_{d1d3}$). We found that the flexible linker was essential for improving the silica binding performance of the $L2_{d1}$-tagged phages, as only $T7_{L\text{-}L2d1}$ phages statistically outperformed wild type T7 ($T7_{wt}$) in terms of the number of phages bound to silica-coated MNPs. This work provides an important step toward overcoming some of the hurdles facing phage-based technologies. Additional work in optimizing L2's assembly on phage capsids and increasing the strength of capsid-directed phage conjugation onto silica surfaces will further improve accessibility of point-of-care detection systems to improve public health and reduce the socioeconomic burden of bacterial contamination in food and water.

MATERIALS AND METHODS

Bacterial Strains, Control Phages, Media, and Growth Conditions. NRGp4, a mutant version of T7 previously engineered by our group[54] to produce bioluminescent reporter enzyme NanoLuc Luciferase (NLuc)[55] upon host infection, was used as "wild type" T7 and is referred to here as $T7_{wt}$. $T7_{wt}$ was propagated in *E. coli* BL21 cells (ATCC BAA-1025), as described below, and was used as the non-L2-tagged phage control during silica-binding experiments. All engineered pET plasmids (pNRG-172, pNRG-177, or pNRG-178) were separately transformed into, and expressed from within, chemically competent One Shot BL21(DE3) *E. coli* cells (Thermo Fisher Scientific, Waltham, MA), with plasmids maintained using 50 μg/mL ampicillin, as described below. All bacterial cultures were grown in LB Miller broth (Thermo Fisher Scientific) at 37 °C with

https://doi.org/10.1021/acsabm.2c00428
ACS Appl. Bio Mater. 2022, 5, 5104−5112

shaking at 90 rpm. A complete list of bacterial strains, plasmids, and T7 phage iterations can be found in Table S1.

Enumeration of all phage stocks was done using standard full plate plaque assays. Briefly, phages were serially diluted in LB broth under sterile conditions. Then, 5 mL of sterile 0.8% LB top agar (Thermo Fisher Scientific) was heated to 55 °C before adding 100 μL of an *E. coli* BL21 overnight culture and 100 μL of diluted phage. The mixture was poured onto plates of fresh LB Miller bottom agar (1.5% agar) and allowed to solidify under a laminar hood before being incubated at 37 °C for 18−24 h. Plaque counts were used to determine the concentration of phages as plaque forming units/mL (pfu/mL), and propagated phages were stored in SM buffer (100 mM NaCl, 8 mM $MgSO_4{\cdot}7H_2O$, 50 mM Tris, pH 7) at 4 °C for no more than 1 month.

Construction of Plasmid pNRG-172. The pET-17b (AddGene 69663-3) plasmid served as the vector backbone of pNRG-172, with tagged capsid proteins expressed using the pET/BL21(DE3) expression system.[56] T7's *g10A* was amplified using T7's genome as a template. NEB's Phusion High Fidelity PCR Master mix (New England Biolabs, Ipswich, MA) was used for PCR amplifications, and corresponding primers were ordered from IDT (Coralville, IA). A reverse primer was designed so that it omitted *g10A*'s endogenous stop codon and forced translation to terminate at the end of L2 domain 1's ($l2_{d1}$) coding region. The first 180 bases of L2 ($l2_{d1}$) were amplified using an in-house plasmid containing BL21(DE3)'s complete L2 gene. The reverse primer used for amplifying L2's domain 1 also added a double stop codon to the end of $l2_{d1}$. Regions of homology were added to the C-terminal of amplicon *g10A* and the N-terminal of amplicon $l2_{d1}$ using PCR and primer overhangs. Assembly was accomplished using NEBuilder HiFi DNA Assembly Master mix (New England Biolabs), and the final recombined construct ("*g10A*-$l2_{d1}$") was amplified using another set of primers to add 5′-*Hin*dIII and 3′-*Bam*HI cut sites to respective ends of the final amplicon. Both the pET-17b vector backbone and the final *g10A*-$l2_{d1}$ fragment were double-digested using *Hin*dIII-HF and *Bam*HI-HF endonucleases purchased from NEB (New England Biolabs) and were subsequently gel purified before being ligated together in a 1:3 (vector to insert) ratio. Ligated plasmids were transformed into *E. coli* BL21(DE3) cells, following manufacturer recommendations, and final plasmids were isolated from single bacterial colonies before being sequenced (Cornell Institute of Biotechnology Core Facilities, Ithaca, NY) to ensure proper plasmid assembly. Figure 1 depicts the pNRG-172 plasmid, and a complete list of primers used to make pNRG-172 can be found in Table S2. Plasmid maps are found in Figure S1.

Construction of Plasmid pNRG-177. Plasmid pNRG-177 expressed the same tagged version of T7's major capsid protein as pNRG-172 expressed, but this iteration also contained a flexible linker placed between Gp10A and $L2_{d1}$. pNRG-177 was constructed using the same double-digested pET-17b backbone that had been used to assemble pNRG-172 and a preassembled gBlock that contained *g10A*, a fusion protein linker,[57] and L2's domain 1 (residues 1−60). pNRG-177's gBlock (IDT) was PCR amplified to add 5′-*Hin*dIII and 3′-*Bam*HI cut sites to respective fragment ends and then was double-digested as described above. Vector and insert were ligated together in a 1:3 ratio, respectively, and final ligated plasmids were transformed into chemically competent *E. coli* BL21(DE3) cells, following manufacturer recommendations. Plasmids were isolated from single bacterial transformant colonies and sequenced to ensure proper assembly of the plasmid. A complete list of primers can be found in Table S2, while all plasmid maps can be found in Figure S1.

Construction of Plasmid pNRG-178. Plasmid pNRG-178 was constructed by ligating the digested pET-17b used previously with a modified version of pNRG-177's gBlock such that it coded for *g10A*, the selected flexible linker, $l2_{d1}$, and L2's domain 3 ($l2_{d3}$). To modify the original gBlock, PCR was used to amplify L2's domain 3 (residues 203−274) using the reverse primer to add a double stop codon to the end of $l2_{d3}$. When amplifying the "*g10A*-linker-$l2_{d1}$" from the original gBlock, the reverse primer used for the respective amplification was omitted, and the double stop codon from the end of $l2_{d1}$ was effectively removed, so that the translation would be terminated after L2's domain 3 had been expressed. HiFi recombination, facilitated by regions of homology added to the ends of each respective amplicon, was used to stitch $l2_{d3}$ to the end of the *g10A*-linker-$l2_{d1}$ amplicon, making the final product "*g10A*-linker-$l2_{d1}l2_{d3}$". Another set of primers added cut sites, 5′-HIndIII and 3′-*Bam*HI, to the assembled insert, and the final product was double-digested as previously described. Ligation was performed in a 1:3 ratio, and plasmids were transformed into chemically competent *E. coli* BL21(DE3) cells as the manufacture guidelines dictated. Plasmids were isolated from single bacterial colonies and sequenced as previously described to ensure proper assembly of the plasmid. A complete list of primers can be found in Table S2, while all plasmid maps can be found in Figure S1.

Propagation of $T7_{wt}$, $T7_{L2d1}$, $T7_{L\text{-}L2d1}$, and $T7_{L\text{-}L2d1d3}$ Phages and Confirmation of Tagged Capsids. Cultures of *E. coli* BL21(DE3) transformed with either plasmid pNRG-172, pNRG-177, or pNRG-178, as well as cultures of *E. coli* BL21 without a plasmid, were grown to an OD_{600} of 0.2 in LB medium (supplemented with 50 μg/mL ampicillin for the *E. coli* cells with plasmids only); then, isopropyl ß-D-1-thiogalactopyranoside (IPTG) was added to a final concentration of 0.5 mM to induce protein expression for 30 min at 37 °C with 90 rpm shaking. Then, Mg^{2+} and Ca^{2+} were added to a final concentration of 1 mM each, and $T7_{wt}$ phages were added with a 0.01 multiplicity of infection at 37 °C and 90 rpm shaking. When there was visible clearance of the culture, cell debris was pelleted by centrifugation (3260*g*, 20 min). Unpurified phages were enumerated using standard plaque assays.

The phage on tap method[58] was used to purify and concentrate the phages by first filtering the unpurified phage solution through a 0.22 μm PVDF filter and then washing half of the filtrate 3 times with SM buffer (100 mM NaCl, 8 mM $MgSO_4{\cdot}7H_2O$, 50 mM Tris, pH 7) and the other half of the filtrate 3 times with PBS using Amicon Ultra-15 centrifugal filter units (100 kDa MWCO cellulose membranes; Millipore Sigma). After the last wash, the phages in SM buffer (100 mM NaCl, 8 mM $MgSO_4{\cdot}7H_2O$, 50 mM Tris, pH 7) were stored at 4 °C for later silica-binding experiments. Separately, phages in PBS had their proteins extracted with 5 freeze−thaw cycles. Then, 50 units of RNase-free DNaseI (Norgen, Thorold, ON, CA) were added, and then, samples were incubated at 37 °C for 2 h.[59]

The extracted proteins were analyzed by SDS-PAGE and Western blot. One part Laemmli buffer (2×; Bio-Rad, Hercules, CA) supplemented with 5% (v/v) 2-mercaptoethanol (Bio-Rad) was added to one part of each sample to a final concentration of 1× Laemmli, and these mixtures were heated at 100 °C for 5 min. Proteins were separated on a 4−20% gradient SDS-PAGE gel (Bio-Rad) at 120 V for ∼1.5 h, and then, the proteins were transferred to an Immobilon-P membrane (Millipore Sigma, Burlington, MA) at 100 V for 1 h. After blocking with 2% BSA for either 1 h (room temperature) or overnight (4 °C), proteins were tagged with a T7-tag polyclonal antibody (1:1000 dilution; Invitrogen, PA1-32386, Waltham, MA) and incubated for 1 h (room temperature). The membranes were washed with TBS three times for 5 min each, and then, the secondary antibody (goat antirabbit alkaline phosphatase; 1:8000 dilution; Invitrogen, G21079) was added and incubated for 1 h (room temperature). The membranes were washed three times with TBS again, and then, tagged proteins were visualized with Novex AP chromogenic substrate (Invitrogen, WP 20001).

Functionalization of $T7_{wt}$, $T7_{L2d1}$, $T7_{L\text{-}L2d1}$, and $T7_{L\text{-}L2d1d3}$ Phages onto Silica-Coated MNPs. Aliquots of the purified and concentrated SM buffer (100 mM NaCl, 8 mM $MgSO_4{\cdot}7H_2O$, 50 mM Tris, pH 7) stocks of $T7_{L2d1}$, $T7_{L\text{-}L2d1}$, $T7_{L\text{-}L2d1d3}$, and $T7_{wt}$ were diluted in Tris binding buffer (10 mM Tris; 0.1% Tween 20; pH = 7.4 or 9) to make ∼5×10^{10} pfu/mL stocks for silica-binding experiments. Based on previous experiments, ∼10^9 magnetized phages per assay were targeted to provide a good capture efficiency.[19] To 100 μL aliquots of the diluted phage stocks was added 0.67 μL of silica-coated magnetic nanoparticles (MNPs; Creative Diagnostics, WHM-X065, Shirley, NY). The stock concentration of MNPs was determined to be 5×10^{12} MNPs/mL by nanoparticle tracking analysis (Cornell NanoScale Science and Technology Facility). Briefly, the MNPs were diluted 100× in water and analyzed with a Malvern NS300 NanoSight instrument. Phage/MNP samples were

https://doi.org/10.1021/acsabm.2c00428
ACS Appl. Bio Mater. 2022, 5, 5104−5112

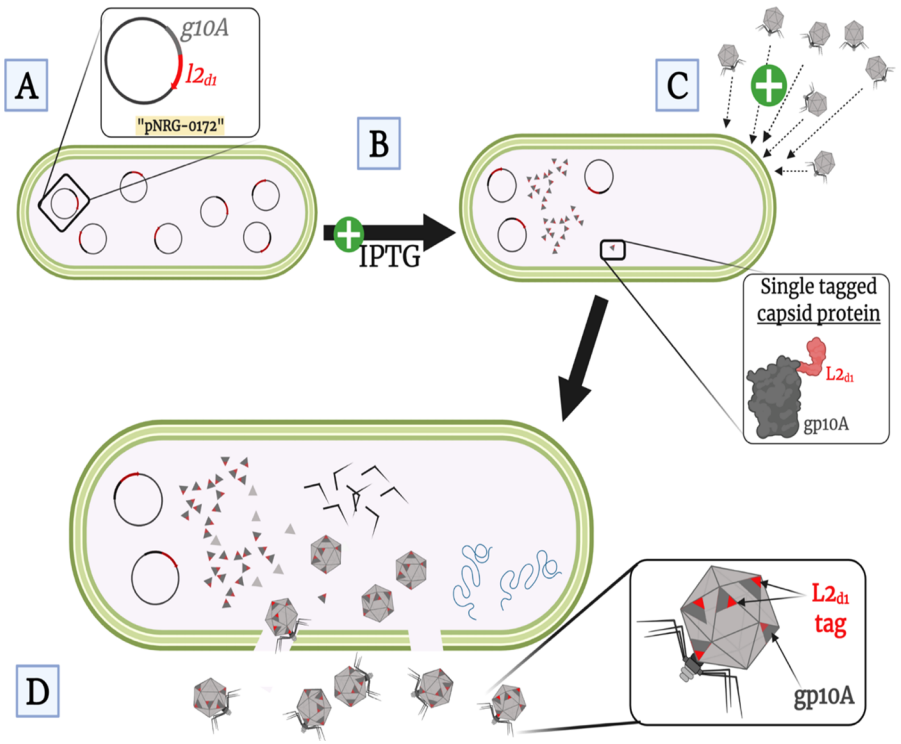

Figure 2. Plasmid-based expression for L2-tagged major capsid proteins. (A) A pET plasmid expression system in *E. coli* DE3 cells expresses T7's major capsid protein (Gp10A) fused to different versions of a silica-binding tag (in this case, $L2_{d1}$) (B) when induced with IPTG. (C) Wild type T7 phages are added; (D) during normal phage infection, pre-expressed Gp10A-$L2_{d1}$ proteins are assembled into T7 capsids, and tagged progeny are released.

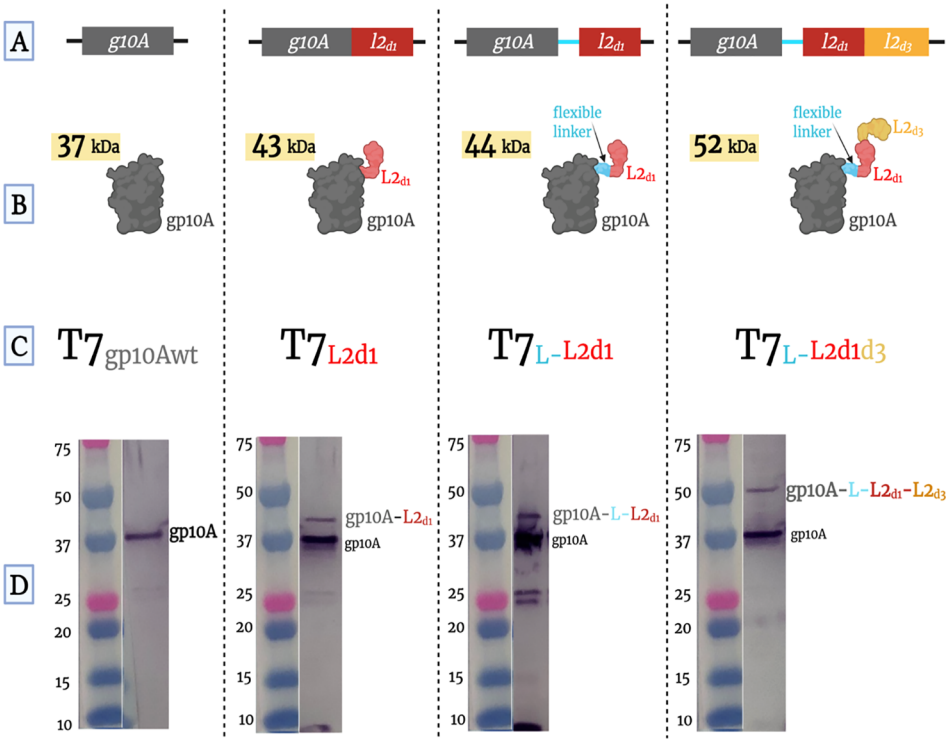

Figure 3. Summary of genetic constructs, proteins, phages, and Western blot characterization. (A) Genetic constructs from which L2-tagged Gp10A protein iterations are expressed. (B) Cartoon representations of these fusion proteins. (C) Names of the T7 phages produced. (D) Corresponding Western blot analyses of denatured phage samples showing the incorporation of the different Gp10A proteins.

rotated at 20 rpm at room temperature (18 °C) for either 15 min or 1 h. Then, the MNPs (with bound phage) were separated using a magnet (BD IMag; BD Biosciences, Franklin Lakes, NJ); the supernatant was removed, and the phage−MNP conjugates were resuspended in 250 μL of Tris binding buffer. This washing procedure was repeated 3 more times, saving the washes each time. After the last

https://doi.org/10.1021/acsabm.2c00428
ACS Appl. Bio Mater. 2022, 5, 5104−5112

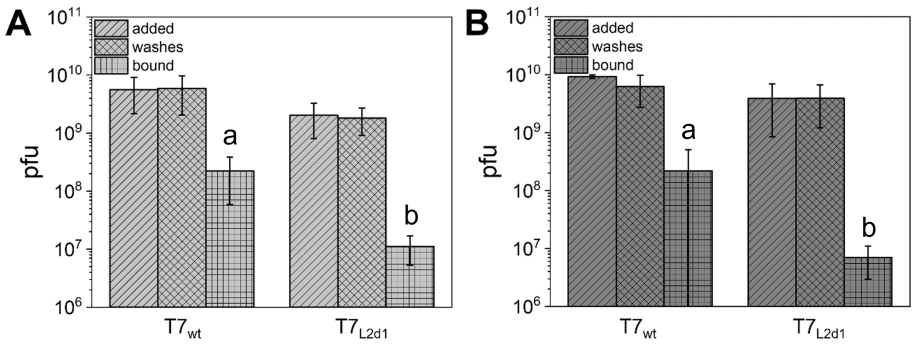

Figure 4. Quantity of phages (pfu) added to the MNPs, in the washes, and bound to the MNPs for $T7_{wt}$ and $T7_{L2d1}$ phages after 15 min of incubation at (A) pH 7.4 or (B) pH 9. The raw data used to construct this figure is shown in Tables S4 and S5. Means of *bound* phage quantities with different letters within a graph are statistically significant ($p < 0.05$). Full statistical analyses are reported in Tables S6–S9. Values represent means (with error bars representing standard deviations) of at least 3 samples enumerated from 3 separate biological replicates ($n \geq 9$).

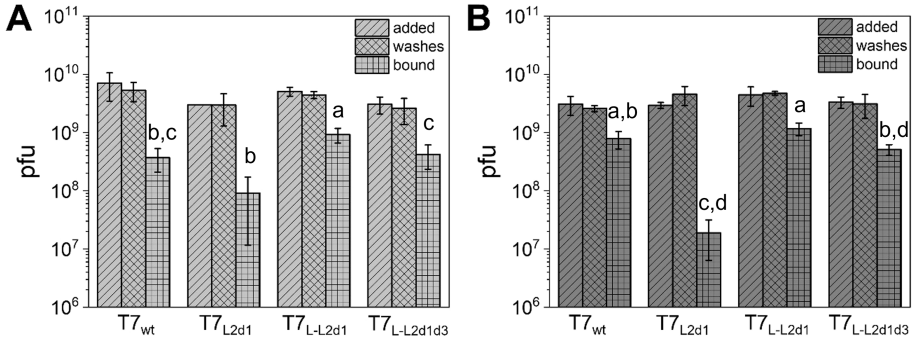

Figure 5. Quantity of phages (pfu) added to the MNPs, in the washes, and bound to the MNPs for $T7_{wt}$, $T7_{L2d1}$, $T7_{L-L2d1}$, and $T7_{L-L2d1d3}$ phages after 1 h of incubation at (A) pH 7.4 or (B) pH 9. The raw data used to construct this figure is shown in Tables S10 and S11. Means of *bound* phage quantities with different letters within a graph are statistically significant ($p < 0.05$). Full statistical analyses are reported in Tables S12–S14. Values represent means (with error bars representing standard deviations) of at least triplicate ($n \geq 3$) replication.

wash, the phage–MNPs were resuspended in 50 μL of Tris binding buffer. Free phages (in the washes), silica-bound phages (in the pellet), and phages in the diluted stocks were enumerated using standard plaque assays. pfu in each sample was calculated by multiplying the plate count by the volume of the sample (100 μL for the stock/"added" sample, 50 μL for the "bound" sample, and 835 μL for the wash sample).

Statistical Analysis. The data were analyzed in jamovi (Sydney, Australia) using ANOVA or one-way ANOVA. The Shapiro–Wilk test was used to check the normality of the data. Levene's test was used to check the homogeneity of variances for the groups being compared. If the variances were found to be equal, Fisher's ANOVA was used. If the variances were found to be unequal, Welch's ANOVA was used. When 3 group means were compared, post hoc tests were used to determine which mean(s) differed from the others. When the variances were equal, the Tukey post hoc test was used. When the variances were unequal, the Games–Howell post hoc test was used. Significance was determined with a cutoff of $p < 0.05$.

RESULTS AND DISCUSSION

Plasmid Design and Expression of L2-Tagged Gp10A Proteins. Many factors can contribute to improving the orientation and performance of phages immobilized to MNPs. Here, the influence of conjugation time, pH value of conjugation solution, composition of silica tag, and presence or absence of linker were explored to maximize the number of L2-tagged T7 phages immobilized to silica-coated MNPs. As depicted in Figure 2, to incorporate L2 into the T7 capsid, we engineered a plasmid (pNRG-172) where the gene for L2 domain 1 ($l2_{d1}$) was translationally fused downstream of *g10A* in place of T7's minor capsid gene, *g10B*. Phage display research commonly targets *g10B* when engineering T7, as this location results in outward-facing tags that decorate the outside of the T7 capsid.[48] In the presence of IPTG, the plasmid expressed a fusion of T7's major capsid protein, Gp10A, and $L2_{d1}$. Then, during $T7_{wt}$ phage infection, Gp10A-$L2_{d1}$ proteins self-assembled onto the phage capsid to produce $T7_{L2d1}$ phages.

The same expression method was used for plasmids pNRG-177 and pNRG-178. Plasmid pNRG-177 expressed Gp10A fused to a hydrophilic flexible linker (GSAGSAAGSGEF)[57] and $L2_{d1}$ (Gp10A-L-$L2_{d1}$). Linkers (short peptides bound between domains of fusion proteins) can improve protein function, increase yield, and promote molecular flexibility during conjugation.[60] Additionally, plasmid pNRG-178 was designed so that Gp10A was fused by the flexible linker mentioned above to both $L2_{d1}$ and $L2_{d3}$, on the basis of prior work in which researchers demonstrated a reduced dissociation constant (and correspondingly increased binding affinity) when green fluorescent protein (GFP) was fused with both domains.[46]

Incorporation of the proteins into the phage capsid was confirmed by Western blots, which presented a band around 43 kDa corresponding to Gp10A-L2d1 for $T7_{L2d1}$ phages (Figure 3, column 2), a band around 44 kDa corresponding to Gp10A-L-$L2_{d1}$ for $T7_{L-L2d1}$ phages (Figure 3, column 3), and a band around 52 kDa corresponding to Gp10A-L-$L2_{d1d3}$ for $T7_{L-L2d1d3}$ phages (Figure 3, column 4). $T7_{wt}$ phages only presented a band for wild type Gp10A, as expected (Figure 3, column 1). Original gels, without any image processing, are

https://doi.org/10.1021/acsabm.2c00428
ACS Appl. Bio Mater. 2022, 5, 5104–5112

available in the Supporting Information (Figure S2). Engineering pNRG-177 separate from pNRG-172 ensured that the ~44 kDa band in the $T7_{L\text{-}L2d1}$ phage sample could be assigned to Gp10A-linker-$L2_{d1}$, despite its size similarity to the Gp10A-$L2_{d1}$ protein produced by pNRG-172. The band for $Gp10A_{wt}$ was more intense than the band for all of the L2-tagged proteins, indicating incorporation of more wild type Gp10A into the phage capsid compared to L2-tagged Gp10A. Several values of IPTG concentration and multiplicity of infection (MOI) were evaluated to optimize the production of Gp10A-L2d1 proteins and their assembly onto $T7_{L2d1}$ phages (see the SI). Briefly, there was no difference in amount of protein expressed as a function of IPTG concentration, so we chose to use 0.5 mM IPTG due to our previous experience using this concentration with pET plasmids. In addition, lower MOIs generally led to higher phage titers and should lead to the production of phages with higher quantities of tagged capsid proteins, so we chose to use a MOI of 0.01 for the production of L2-tagged T7 phages.

Influence of Time on L2-Tagged T7 Phage Binding to Silica-Coated MNPs. $T7_{L2d1}$ and $T7_{wt}$ phages were incubated with silica-coated MNPs at pH 7.4 for 15 min and 1 h (Figures 4A and 5A, full statistical analyses of all binding experiments are available in Tables S6−S14). After 1 h, there were significantly more phages of both types bound to the silica-coated MNPs, so all subsequent experiments were conducted for 1 h to give the phages more time to adsorb. However, after the 1 h incubation, there was not a significant difference between the number of $T7_{L2d1}$ phages bound to the MNPs, compared to $T7_{wt}$ phages, meaning that $L2_{d1}$ on its own was not increasing the affinity of the tagged phages for silica compared to the wild type phages. These results were unexpected and in contrast to a prior report in which GFP tagged with $L2_{d1}$ adsorbed to silica with a relatively low dissociation constant.[46] We hypothesize that the maturation process for the $T7_{L2d1}$ capsids may be limiting the molecular flexibility of the $L2_{d1}$ tags and forcing them into unfavorable positions that are unable to adequately adsorb to the silica surfaces.[44]

Influence of Flexible Linker on L2-Tagged T7 Phage Binding to Silica-Coated MNPs. The addition of the flexible linker resulted in a significantly greater number of $T7_{L\text{-}L2d1}$ phages bound to the MNPs compared to both $T7_{L2d1}$ and $T7_{wt}$ phages (Figure 5A, full statistical analyses of all binding experiments are available in Tables S6−S14). The increased number of phages bound for $T7_{L\text{-}L2d1}$ versus $T7_{L2d1}$ suggests that the flexible linker improves molecular flexibility and thus infectivity of the bound phages. We hypothesize that the flexible linker allows more freedom for orientation allowing the phage tail fibers (6 total) to align better with the surface of the bacterium. Indeed, the tail fibers on T7 are relatively short in comparison to other larger phages and therefore they have less reach. Proper injection of DNA requires a near perpendicular alignment of the phage injection apparatus and bacterial surface, an alignment more likely in a phage bound via a flexible versus a nonflexible linker.

Influence of $L2_{d3}$ on T7 Phage Binding to Silica-Coated MNPs. While prior work suggests that including both $L2_{d1}$ and $L2_{d3}$ should reduce the dissociation constant of the protein,[46] in this work, the addition of $L2_{d3}$ did not improve the silica binding behavior of $T7_{L\text{-}L2d1d3}$ phages compared to that of $T7_{L\text{-}L2d1}$. In fact, at pH 7.4, there was not a statistically significant difference in the number of $T7_{L\text{-}L2d1d3}$ bound to silica-coated MNPs compared to $T7_{wt}$ phages (Figure 5A, full statistical analyses of all binding experiments are available in Tables S6−S14). We hypothesize that the addition of $L2_{d3}$ did not result in more phages bound to the MNPs due to the complication of adding a longer tag with multiple silica binding domains to phage capsids. The Gp10A-$L2_{d1d3}$ may not have been able to easily assume favorable conformations for binding to silica, and there may have been fewer modified Gp10A proteins on the $T7_{L\text{-}L2d1d3}$ phages due to the $L2_{d1d3}$ tag being twice as large as $L2_{d1}$. While previous work demonstrated that the strongest affinity toward silica was found when GFP was tagged with all three L2 domains,[46] we hypothesized that tagging Gp10A with all three domains of L2 may have resulted in even fewer modified Gp10A proteins being incorporated during capsid assembly, as T7 phages have previously been shown to incorporate fewer tagged capsid proteins as their fused tags become larger in size.

Influence of pH Value on L2-Tagged T7 Phage Binding to Silica-Coated MNPs. In addition to pH 7.4, all of the L2-tagged phage variations were also incubated at pH 9.0, on the basis of prior work that demonstrated that increasing the pH value improves binding of L2 to silica as a result of the deprotonation of more silanol groups on silica.[44,46] Interestingly, increasing the pH to 9.0 for a 1 h incubation (Figure 5B, full statistical analyses of all binding experiments are available in Tables S6−S14) did not increase the number of phages bound to MNPs for any of the L2-tagged phage types by a statistically significant amount. While this observation contrasts with prior reports, we hypothesize that the introduction of multiple L2-tagged capsid protein across the T7 capsid resulted in increased positive charge imparting charge repulsion between adjacent T7 preventing tighter packing. Alternatively, it may be that the size of the T7 phage (larger than the previous reports investigating L2 alone, or L2 bound to carbonic anhydrase or green fluorescent protein) was the dominating factor in limiting immobilization yield.

CONCLUSION

We successfully used a plasmid-based engineering method to produce T7 phages that incorporated silica-binding tags ($L2_{d1}$ or $L2_{d1d3}$) into their capsids, with and without the integration of a flexible linker peptide. Unlike previous methods that immobilized phages onto silica surfaces, our method ensured that the phages were immobilized to the silica-coated MNPs through their capsids as a result of the capsid L2 tag, which allows the tail fibers to remain unobstructed and available for bacterial detection. Importantly, this work demonstrates the engineering of bacteriophages without postassembly modification, where the genotype and phenotype are not in agreement. In combination with other methods such as gene silencing, phages can be constructed which have the same genotype but largely differing phenotype from their progeny produced in wild type bacteria. Overall, our results showed that MNPs retained a statistically significantly higher quantity of $T7_{L\text{-}L2d1}$ phages compared to $T7_{L2d1}$, $T7_{L\text{-}L2d1d3}$, or $T7_{wt}$ phages, which demonstrates the importance of molecular flexibility in the interaction of capsid-bound L2 tags with silica. Although the overall effect of the L2 tag on silica binding was relatively low, the plasmid-based method for tagging phage capsids demonstrated here could be used for a wide range of tags for other materials. As genetically modified organisms are defined by alterations in their genome, the demonstrated

https://doi.org/10.1021/acsabm.2c00428
ACS Appl. Bio Mater. 2022, 5, 5104−5112

method can allow the *in vivo* capsid modification of phages while maintaining their wild type genome. Future studies on the binding affinity and efficiency of L2 tag modified phages on the basis of linker type would reveal additional practical information. These applications can be used in the biomedical field where the bacteriocidal properties of phages on medical equipment (e.g., catheters) are sought. This work also advances knowledge of using plasmid-based engineering strategies to introduce flexible linkers and fusion peptides to proteins that would benefit from oriented self-assembly onto materials. Thus, our work provides an important step toward the design of future phage-based tools for detection and therapeutics and other site-directed protein immobilization technologies for environmental remediation and biocatalysis.

■ ASSOCIATED CONTENT

Supporting Information

The Supporting Information is available free of charge at https://pubs.acs.org/doi/10.1021/acsabm.2c00428.

List of the bacterial strains, bacteriophages, and plasmids used in this study; list of primers used for plasmid designs and sequencing fragments; titers of T7L2d1 and T7wt phages produced at various MOI values; raw data for Figure 4A,B; results of statistical tests for "bound" data shown in Figure 4; raw data for Figure 5A,B; results of statistical tests for "bound" data shown in Figure 5; sequence maps of all modified pET plasmids; and Western blot showing expression of Gp10A-L2$_{d1}$ (PDF)

■ AUTHOR INFORMATION

Corresponding Author

Sam R. Nugen − *Department of Food Science, Cornell University, Ithaca, New York 14853, United States;* orcid.org/0000-0003-3638-1776; Email: snugen@cornell.edu

Authors

Kathryn A. Hufziger − *Department of Food Science, Cornell University, Ithaca, New York 14853, United States*

Emma L. Farquharson − *Department of Food Science, Cornell University, Ithaca, New York 14853, United States*

Brenda G. Werner − *Department of Food Science, Cornell University, Ithaca, New York 14853, United States*

Qingmin Chen − *Department of Food Science, Cornell University, Ithaca, New York 14853, United States*

Julie M. Goddard − *Department of Food Science, Cornell University, Ithaca, New York 14853, United States;* orcid.org/0000-0002-3644-0732

Complete contact information is available at: https://pubs.acs.org/10.1021/acsabm.2c00428

Author Contributions

†K.A.H. and E.L.F. contributed equally to this work and share first authorship on this manuscript.

Notes

The authors declare no competing financial interest.

■ ACKNOWLEDGMENTS

This work was supported in part by the National Institute of Biomedical Imaging and Bioengineering (NIBIB) R01EB027895 and in part from the United States Department of Agriculture National Institute of Food and Agriculture predoctoral fellowship 2018-07728 and Hatch NYC-143802. This work was performed in part at the Cornell NanoScale Facility, a member of the National Nanotechnology Coordinated Infrastructure (NNCI), which is supported by the National Science Foundation (Grant NNCI-2025233). This work made use of the Cornell Center for Materials Research Shared Facilities which are supported through the NSF MRSEC program (DMR-1719875). Sequencing was performed by the Biotechnology Resource Center (BRC) Genomics Facility (RRID:SCR_021727) at the Cornell Institute of Biotechnology. The authors gratefully acknowledge the Cornell Statistical Consulting Unit and Elizabet Moreno Reyes with support of statistical analysis of the data.

■ REFERENCES

(1) Richter, Ł.; Janczuk-Richter, M.; Niedziółka-Jönsson, J.; Paczesny, J.; Hołyst, R. Recent Advances in Bacteriophage-Based Methods for Bacteria Detection. *Drug Discovery Today* **2018**, *23* (2), 448−455.

(2) Buzby, J. C.; Roberts, T. The Economics of Enteric Infections: Human Foodborne Disease Costs. *Gastroenterology* **2009**, *136* (6), 1851−1862.

(3) World Health Organization. *Food Safety Fact Sheet*, 2020. https://www.who.int/news-room/fact-sheets/detail/food-safety (accessed 10/22/21).

(4) World Health Organization. *Who Estimates of the Global Burden of Foodborne Diseases: Foodborne Disease Burden Epidemiology Reference Group 2007−2015*, 9789241565165, 2015. https://apps.who.int/iris/handle/10665/199350.

(5) Capita, R.; Alonso-Calleja, C. Antibiotic-Resistant Bacteria: A Challenge for the Food Industry. *Crit. Rev. Food Sci.* **2013**, *53* (1), 11−48.

(6) Payne, M. J.; Kroll, R. G. Methods for the Separation and Concentration of Bacteria from Foods. *Trends Food Sci. Technol.* **1991**, *2*, 315−319.

(7) Suh, S. H.; Jaykus, L.-A. Nucleic Acid Aptamers for Capture and Detection of Listeria Spp. *J. Biotechnol.* **2013**, *167* (4), 454−461.

(8) World Health Organization. *Drinking-Water Fact Sheet*, 2019. https://www.who.int/news-room/fact-sheets/detail/drinking-water (accessed 10/22/21).

(9) Xie, X.; Bahnemann, J.; Wang, S.; Yang, Y.; Hoffmann, M. R. Nanofiltration" Enabled by Super-Absorbent Polymer Beads for Concentrating Microorganisms in Water Samples. *Sci. Rep. - UK* **2016**, *6* (1), 20516.

(10) Jaffee, S.; Henson, S.; Unnevehr, L.; Grace, D.; Cassou, E. *The Safe Food Imperative: Accelerating Progress in Low- and Middle-Income Countries*; World Bank: Washington, DC, 2019.

(11) Scharff, R. L. Economic Burden from Health Losses Due to Foodborne Illness in the United States. *J. Food Protect.* **2012**, *75* (1), 123−131.

(12) Hussain, M. A.; Dawson, C. O. Economic Impact of Food Safety Outbreaks on Food Businesses. *Foods* **2013**, *2* (4), 585−589.

(13) de W. Blackburn, C., Ed. *Food Spoilage Microorganisms*; CRC Press LLC: Boca Raton, FL, 2006.

(14) Ross, A.; Ward, S.; Hyman, P. More Is Better: Selecting for Broad Host Range Bacteriophages. *Front. Microbiol.* **2016**, *7*, 1352.

(15) Schmelcher, M.; Loessner, M. J. Application of Bacteriophages for Detection of Foodborne Pathogens. *Bacteriophage* **2014**, *4* (2), No. e28137.

(16) Bertin, A.; de Frutos, M.; Letellier, L. Bacteriophage-Host Interactions Leading to Genome Internalization. *Curr. Opin. Microbiol.* **2011**, *14* (4), 492−496.

(17) Moldovan, R.; Chapman-McQuiston, E.; Wu, X. L. On Kinetics of Phage Adsorption. *Biophys. J.* **2007**, *93* (1), 303−315.

(18) Rakhuba, D.; Kolomiets, E.; Dey, E. S.; Novik, G. Bacteriophage Receptors, Mechanisms of Phage Adsorption and Penetration into Host Cell. *Polym. J. Microbiol.* **2010**, *59* (3), 145.

(19) Zurier, H. S.; Duong, M. M.; Goddard, J. M.; Nugen, S. R. Engineering Biorthogonal Phage-Based Nanobots for Ultrasensitive, in Situ Bacteria Detection. *ACS Appl. Bio Mater.* **2020**, *3* (9), 5824−5831.
(20) Stevens, K. A.; Jaykus, L.-A. Bacterial Separation and Concentration from Complex Sample Matrices: A Review. *Crit. Rev. Microbiol.* **2004**, *30* (1), 7−24.
(21) Machera, S. J.; Niedziółka-Jönsson, J.; Szot-Karpińska, K. Phage-Based Sensors in Medicine: A Review. *Chemosensors* **2020**, *8* (3), 61.
(22) Farooq, U.; Ullah, M. W.; Yang, Q.; Wang, S. Applications of Phage-Based Biosensors in the Diagnosis of Infectious Diseases, Food Safety, and Environmental Monitoring. In *Biosensors for Environmental Monitoring*, Rinken, T., Kivirand, K., Eds.; IntechOpen: London, UK, 2019; pp 175−192.
(23) Gourkhede, D. P.; Wankhade, P. R.; Prasastha, V.; Ram, S. K.; Sakhare, D. T.; Jagannath, A. Application of Bacteriophages in Food Industry: A Review. *International Journal of Livestock Research* **2020**, *10* (9), 1−7.
(24) Xu, J.; Chau, Y.; Lee, Y.-k. Phage-Based Electrochemical Sensors: A Review. *Micromachines* **2019**, *10* (12), 855.
(25) Chen, J.; Andler, S. M.; Goddard, J. M.; Nugen, S. R.; Rotello, V. M. Integrating Recognition Elements with Nanomaterials for Bacteria Sensing. *Chem. Soc. Rev.* **2017**, *46* (5), 1272−1283.
(26) Anany, H.; Chou, Y.; Cucic, S.; Derda, R.; Evoy, S.; Griffiths, M. W. From Bits and Pieces to Whole Phage to Nanomachines: Pathogen Detection Using Bacteriophages. *Annu. Rev. Food Sci. Technol.* **2017**, *8* (1), 305−329.
(27) Mathieu, J.; Yu, P.; Zuo, P.; Da Silva, M. L. B.; Alvarez, P. J. J. Going Viral: Emerging Opportunities for Phage-Based Bacterial Control in Water Treatment and Reuse. *Acc. Chem. Res.* **2019**, *52* (4), 849−857.
(28) Endersen, L.; Coffey, A. The Use of Bacteriophages for Food Safety. *Curr. Opin. Food Sci.* **2020**, *36*, 1−8.
(29) Paczesny, J.; Richter, Ł.; Hołyst, R. Recent Progress in the Detection of Bacteria Using Bacteriophages: A Review. *Viruses* **2020**, *12* (8), 845.
(30) Laube, T.; Cortés, P.; Llagostera, M.; Alegret, S.; Pividori, M. I. Phagomagnetic Immunoassay for the Rapid Detection of Salmonella. *Appl. Microbiol. Biotechnol.* **2014**, *98* (4), 1795−1805.
(31) Wang, D.; Hinkley, T.; Chen, J.; Talbert, J. N.; Nugen, S. R. Phage Based Electrochemical Detection of Escherichia Coli in Drinking Water Using Affinity Reporter Probes. *Analyst* **2019**, *144* (4), 1345−1352.
(32) Chen, J.; Alcaine, S. D.; Jiang, Z.; Rotello, V. M.; Nugen, S. R. Detection of *Escherichia coli* in Drinking Water Using T7 Bacteriophage-Conjugated Magnetic Probe. *Anal. Chem.* **2015**, *87* (17), 8977−8984.
(33) Janczuk, M.; Richter, Ł.; Hoser, G.; Kawiak, J.; Łoś, M.; Niedziółka-Jönsson, J.; Paczesny, J.; Hołyst, R. Bacteriophage-Based Bioconjugates as a Flow Cytometry Probe for Fast Bacteria Detection. *Bioconjugate Chem.* **2017**, *28* (2), 419−425.
(34) Tolba, M.; Minikh, O.; Brovko, L. Y.; Evoy, S.; Griffiths, M. W. Oriented Immobilization of Bacteriophages for Biosensor Applications. *Appl. Environ. Microbiol.* **2010**, *76* (2), 528−535.
(35) Wang, Z.; Wang, D.; Chen, J.; Sela, D. A.; Nugen, S. R. Development of a Novel Bacteriophage Based Biomagnetic Separation Method as an Aid for Sensitive Detection of Viable Escherichia Coli. *Analyst* **2016**, *141* (3), 1009−1016.
(36) Edgar, R.; McKinstry, M.; Hwang, J.; Oppenheim, A. B.; Fekete, R. A.; Giulian, G.; Merril, C.; Nagashima, K.; Adhya, S. High-Sensitivity Bacterial Detection Using Biotin-Tagged Phage and Quantum-Dot Nanocomplexes. *P. Natl. Acad. Sci. USA* **2006**, *103* (13), 4841−4845.
(37) Imai, M.; Mine, K.; Tomonari, H.; Uchiyama, J.; Matuzaki, S.; Niko, Y.; Hadano, S.; Watanabe, S. Dark-Field Microscopic Detection of Bacteria Using Bacteriophage-Immobilized Sio2@Aunp Core-Shell Nanoparticles. *Anal. Chem.* **2019**, *91* (19), 12352−12357.
(38) Liana, A. E.; Marquis, C. P.; Gunawan, C.; Gooding, J. J.; Amal, R. T4 Bacteriophage Conjugated Magnetic Particles for E. Coli Capturing: Influence of Bacteriophage Loading, Temperature and Tryptone. *Colloid Surface B* **2017**, *151*, 47−57.
(39) Carmody, C. M.; Goddard, J. M.; Nugen, S. R. Bacteriophage Capsid Modification by Genetic and Chemical Methods. *Bioconjugate Chem.* **2021**, *32* (3), 466−481.
(40) United Nations, Department of Economic and Social Affairs, Population Division. *World Population Prospects 2019: Highlights*; ST/ESA/SER.A/423; UN, New York, NY, 2019.
(41) Cademartiri, R.; Anany, H.; Gross, I.; Bhayani, R.; Griffiths, M.; Brook, M. A. Immobilization of Bacteriophages on Modified Silica Particles. *Biomaterials* **2010**, *31* (7), 1904−1910.
(42) Bone, S.; Alum, A.; Markovski, J.; Hristovski, K.; Bar-Zeev, E.; Kaufman, Y.; Abbaszadegan, M.; Perreault, F. Physisorption and Chemisorption of T4 Bacteriophages on Amino Functionalized Silica Particles. *J. Colloid Interface Sci.* **2018**, *532*, 68−76.
(43) Bhardwaj, N.; Bhardwaj, S.; Devi, P.; Dahiya, S.; Singla, M.; Ghanshyam, C.; Minakshi, P. Phage Immobilized Antibacterial Silica Nanoplatform: Application against Bacterial Infections. *Adv. Anim. Vet. Sci.* **2015**, *3* (1s), 1−9.
(44) Tosaka, R.; Yamamoto, H.; Ohdomari, I.; Watanabe, T. Adsorption Mechanism of Ribosomal Protein L2 onto a Silica Surface: A Molecular Dynamics Simulation Study. *Langmuir* **2010**, *26* (12), 9950−9955.
(45) Kim, S.; Joo, K. I.; Jo, B. H.; Cha, H. J. Stability-Controllable Self-Immobilization of Carbonic Anhydrase Fused with a Silica-Binding Tag onto Diatom Biosilica for Enzymatic Co2 Capture and Utilization. *ACS Appl. Mater. Interfaces* **2020**, *12* (24), 27055−27063.
(46) Taniguchi, K.; Nomura, K.; Hata, Y.; Nishimura, T.; Asami, Y.; Kuroda, A. The Si-Tag for Immobilizing Proteins on a Silica Surface. *Biotechnol. Bioeng.* **2007**, *96* (6), 1023−1029.
(47) Ikeda, T.; Kuroda, A. Why Does the Silica-Binding Protein "Si-Tag" Bind Strongly to Silica Surfaces? Implications of Conformational Adaptation of the Intrinsically Disordered Polypeptide to Solid Surfaces. *Colloid Surface B* **2011**, *86* (2), 359−363.
(48) Deng, X.; Wang, L.; You, X.; Dai, P.; Zeng, Y. Advances in the T7 Phage Display System (Review). *Mol. Med. Rep.* **2017**, *17* (1), 714−720.
(49) Qimron, U.; Tabor, S.; Richardson, C. C. New Details About Bacteriophage T7-Host Interactions-Researchers Are Showing Renewed Interest in Learning How Phage Interact with Bacterial Hosts, Adapting to and Overcoming Their Defenses. *Microbe* **2013**, *5* (3), 117.
(50) Heineman, R. H.; Bull, J. J. Testing Optimality with Experimental Evolution: Lysis Time in a Bacteriophage. *Evolution: International Journal of Organic Evolution* **2007**, *61* (7), 1695−1709.
(51) Shin, J.; Jardine, P.; Noireaux, V. Genome Replication, Synthesis, and Assembly of the Bacteriophage T7 in a Single Cell-Free Reaction. *ACS Synth. Biol.* **2012**, *1* (9), 408−413.
(52) Calendar, R., Ed. *The Bacteriophages: Vol. 1*; Springer Science & Business Media: New York, NY, 2012.
(53) Jończyk, E.; Kłak, M.; Międzybrodzki, R.; Górski, A. The Influence of External Factors on Bacteriophages—Review. *Folia Microbiologica* **2011**, *56* (3), 191−200.
(54) Hinkley, T. C.; Singh, S.; Garing, S.; Le Ny, A.-L. M.; Nichols, K. P.; Peters, J. E.; Talbert, J. N.; Nugen, S. R. A Phage-Based Assay for the Rapid, Quantitative, and Single Cfu Visualization of E. Coli (Ecor #13) in Drinking Water. *Sci. Rep. - UK* **2018**, *8* (1), 14630.
(55) Hall, M. P.; Unch, J.; Binkowski, B. F.; Valley, M. P.; Butler, B. L.; Wood, M. G.; Otto, P.; Zimmerman, K.; Vidugiris, G.; Machleidt, T.; Robers, M. B.; Benink, H. A.; Eggers, C. T.; Slater, M. R.; Meisenheimer, P. L.; Klaubert, D. H.; Fan, F.; Encell, L. P.; Wood, K. V. Engineered Luciferase Reporter from a Deep Sea Shrimp Utilizing a Novel Imidazopyrazinone Substrate. *ACS Chem. Biol.* **2012**, *7* (11), 1848−1857.
(56) Pan, S.-h.; Malcolm, B. A. Reduced Background Expression and Improved Plasmid Stability with Pet Vectors in Bl21 (De3). *Biotechniques* **2000**, *29* (6), 1234−1238.

https://doi.org/10.1021/acsabm.2c00428
ACS Appl. Bio Mater. 2022, 5, 5104−5112

(57) Waldo, G. S.; Standish, B. M.; Berendzen, J.; Terwilliger, T. C. Rapid Protein-Folding Assay Using Green Fluorescent Protein. *Nat. Biotechnol.* **1999**, *17* (7), 691−695.
(58) Bonilla, N.; Rojas, M. I.; Netto Flores Cruz, G.; Hung, S.-H.; Rohwer, F.; Barr, J. J. Phage on Tap-a Quick and Efficient Protocol for the Preparation of Bacteriophage Laboratory Stocks. *PeerJ.* **2016**, *4*, No. e2261.
(59) Boulanger, P. Purification of Bacteriophages and Sds-Page Analysis of Phage Structural Proteins from Ghost Particles. In *Bacteriophages Methods and Protocols, Vol. 2: Molecular and Applied Aspects*; Clokie, M. R. J., Kropinski, A. M., Eds.; Humana Press: 2009; Vol. 2, pp 227−238.
(60) Chen, X.; Zaro, J. L.; Shen, W.-C. Fusion Protein Linkers: Property, Design and Functionality. *Adv. Drug Deliver. Rev.* **2013**, *65* (10), 1357−1369.

https://doi.org/10.1021/acsabm.2c00428
ACS Appl. Bio Mater. 2022, 5, 5104−5112